Supporting Information:

Flat Phonon Bands based Mechanism of Amorphization of MOF-5 at *Ultra-low* Pressures

Meha Bhogra and Umesh V. Waghmare*

Theoretical Sciences Unit, Jawaharlal Nehru Centre for Advanced Scientific Research, Jakkur, Bangalore 560 064, India

E-mail: waghmare@jncasr.ac.in

Phone: +91.80.2208.2842. Fax: +91.80.2208.2767

Crystal structure of MOF-5

The starting structure of MOF-5 crystal considered for this study is obtained from Ref.[S1] The relaxed structure obtained from our *first-principles* DFT calculations at zero pressure is provided at the end of this document.

MOF-5 exists in a face-centered cubic structure and consists of secondary building units (SBUs) positioned at the Bravais sites connected by benzene linkers along $\langle 100 \rangle$ directions (Figure S1). The *fcc* structure with $Fm\bar{3}m$ symmetry is corroborated by simulated XRD pattern showing high peak-intensity for (110), (121) and (220) peaks.

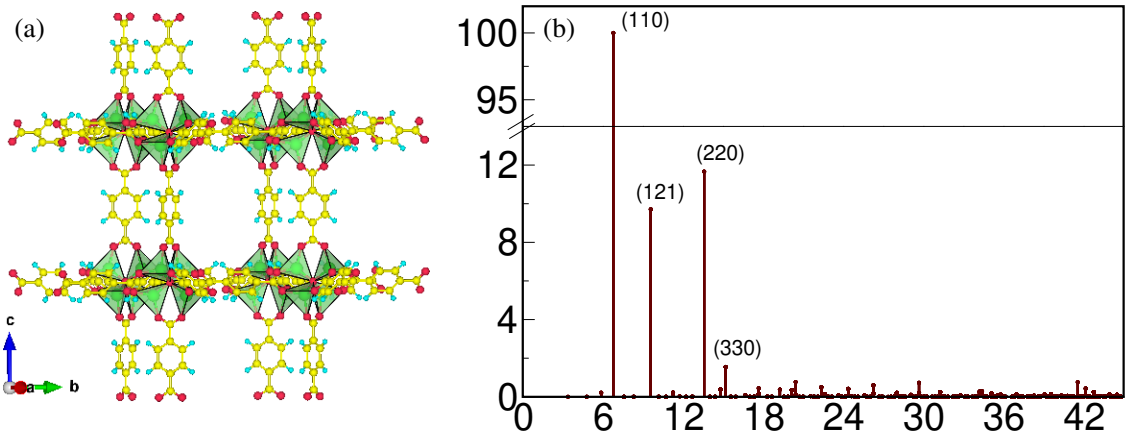

Figure S1: (a) Cubic structure of MOF-5 crystal viewed along [110] direction. Adjacent SBUs are rotated by 90^o about each other, and are bonded through organic linkers (i.e. benzene rings) along $\langle 100 \rangle$. Dashed box delineates the 1,4-benzodicarboxylate or the BDC group,[S2] and (b) simulated XRD shows high peak-intensity primarily along (110), (121), (220) planes, and the corresponding q-values agree closely with the experimental observations for single-crystal MOF-5.[S3]

Frequencies and irreps of the low-energy normal modes of bulk and strained (ε_h = -0.003) MOF-5 structures, along with symmetry of the structures they generate are detailed in Table S1.

Table S1: Frequencies and symmetry labels of low-frequency phonon modes of bulk MOF-5 subjected to compressive strains; ε_h = 0.0 and ε_h = -0.003. Column III shows the subgroups of $Fm\bar{3}m$ generated by the symmetry labels (Column IV) of the normal modes of MOF-5 crystal.

ε_h = 0.0	ε_h = -0.003	Resulting	Irrep
ω (THz)	ω (THz)	structure	
3.1	-1.7	P-1 (2)	T_{1g}
3.1	-1.7	P-1 (2)	
3.1	-1.7	C2/m (12)	
1.6	-1.4	C2 (5)	T_{2u}
1.6	-1.4	C2 (5)	
1.6	-1.4	Imm2 (44)	
2.9	-1.2	P-1 (2)	T_{2g}
2.9	-1.2	P-1 (2)	
2.9	-1.2	C2/m (12)	
1.5	0.4	P1 (1)	T_{1u}
1.5	0.4	Cm (8)	
1.5	0.4	P1 (1)	
0.6	1.1	Fm-3 (202)	A_{2g}
1.4	1.2	C2 (5)	T_{2u}
1.4	1.2	C2 (5)	
1.4	1.2	Imm2 (44)	
0.7	1.3	P-1 (2)	T_{1g}
0.7	1.3	P-1 (2)	
0.7	1.3	C2/m (12)	
0.8	1.4	Fmmm (69)	E_g
0.8	1.4	I4/mmm (139)	

Structural instability of MOF-5 crystal upon expansion

At ε_h = 0.01, the MOF-5 structure undergoes a lattice instability, as characterized by unstable optical modes in its vibrational spectrum (Figure S2).

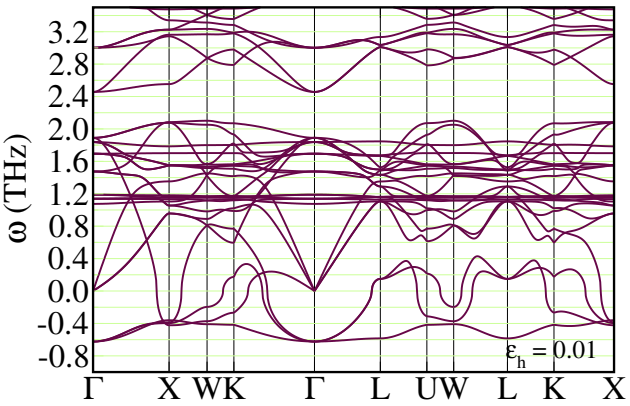

Figure S2: Low-frequency vibrational spectrum of expanded MOF-5 crystal, $\varepsilon_h = 0.01$, exhibiting unstable optical phonon bands.

Nature of normal modes of MOF-5 that destabilize the SBUs on compression

At very small compressive strains $\varepsilon_h \sim$ -0.003, MOF-5 crystal undergoes lattice instabilities. The unstable phonon modes show maximum overlap with normal modes of bulk MOF-5 in the mid-frequency range, $\omega \in \{1.6\text{-}3.2\ \text{THz}\}$. The corresponding eigen-vectors show rotation and in-plane displacements of the BDC groups, as shown in Figure S3.

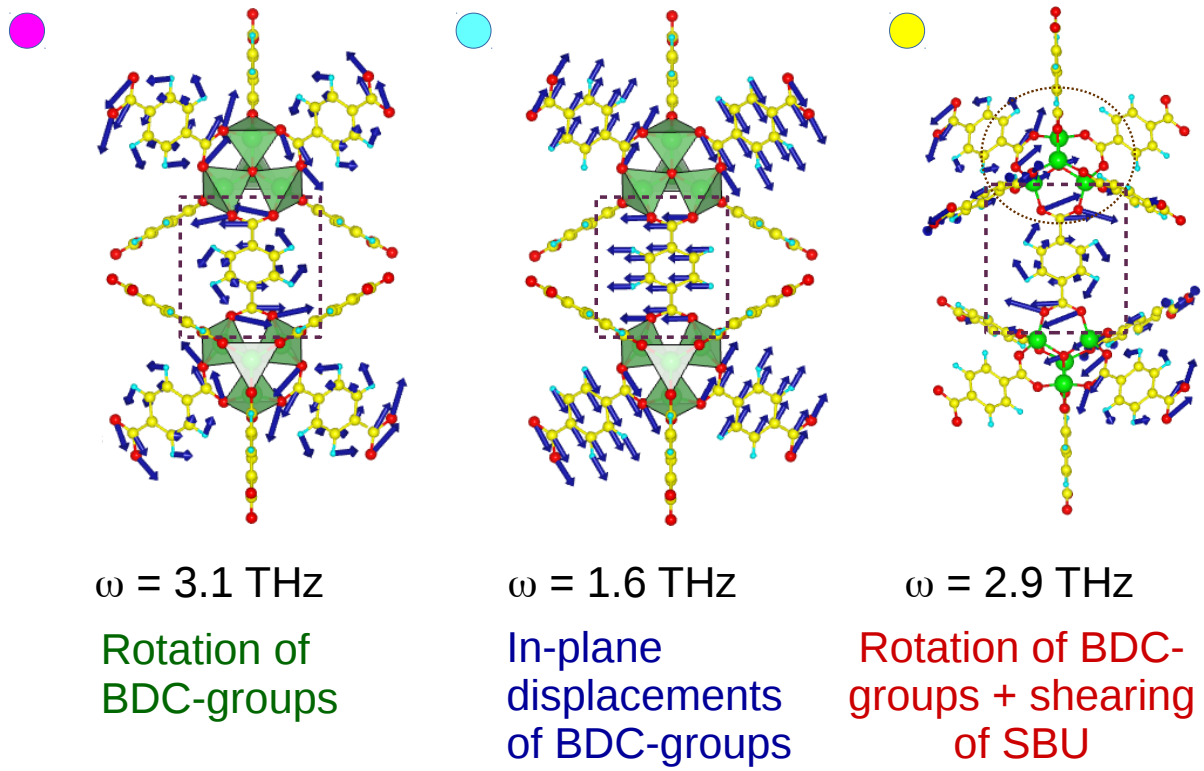

Figure S3: Eigenvectors of normal modes in frequency range $\omega \sim \{1.6\text{-}3.1\ \text{THz}\}$ that become unstable at $\varepsilon_h \sim -0.003$.

Freezing-in these normal modes in strained MOF-5 crystals shows harmonic dependence of strain-energy $E(\varepsilon_h, u_\nu) - E(\varepsilon_h, u_\nu=0)$ on amplitudes u_ν for $|\varepsilon_h| < 0.3\%$ to quartic in u_ν for $|\varepsilon_h| \geq 0.3\%$ (Figure S4).

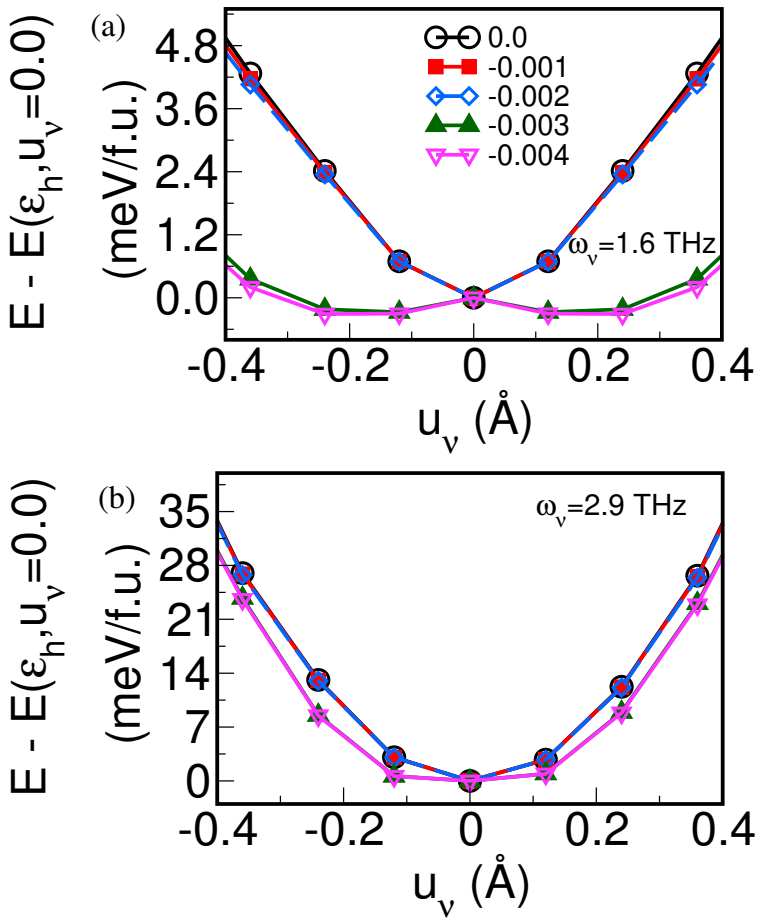

Figure S4: Dependence of internal strain energy on amplitude $|u_\nu|$ of triply degenerate modes at (a) ω = 1.6 THz and (b) ω = 2.9 THz.

Relaxation of structural distortions in compressed MOF-5

At low compressive strains, $|\varepsilon_h| < 0.01$, the structures distorted with random combinations of modes in flat unstable phonon bands relax to lower-energy states, and exhibit localized atomic displacements with respect to pristine MOF-5 crystal (Figure S5(a)). However, at moderately larger compressive strains $|\varepsilon_h| > 0.015$, relaxation of structural distortions in MOF-5 crystal give rise to sliding of nano-scaled domains relative to each other and structural inhomogeneities, leading to its irreversible amorphization (Figure S5(b)).

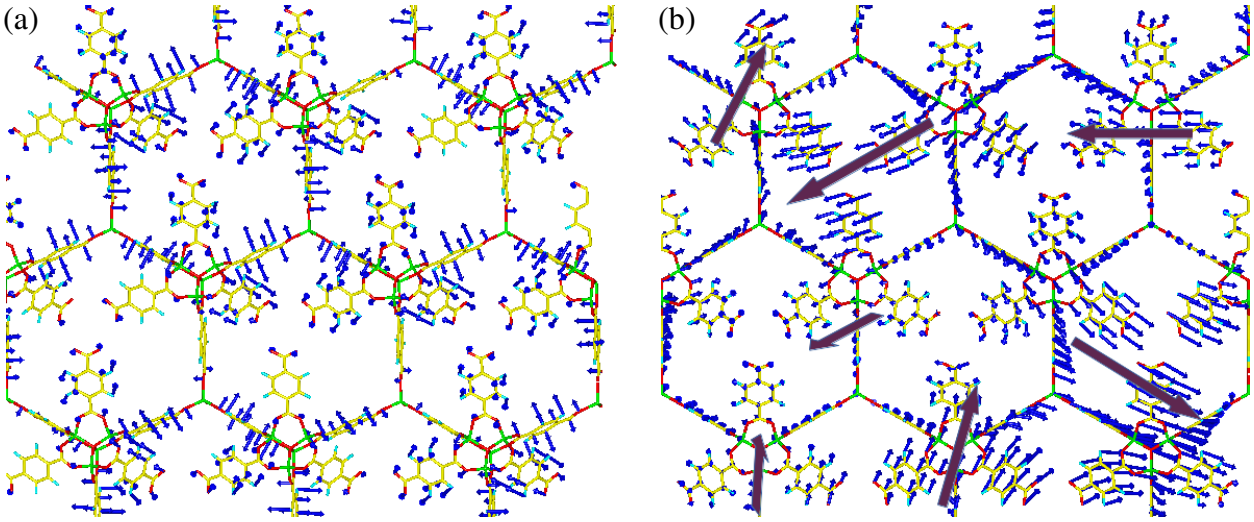

Figure S5: Atomic structural changes in distorted (3 x 3 x 3) supercells optimized to minimum-energy configuration with respect to pristine MOF-5 cyrstal: (a) low-strain regime, ε_h = -0.003, showing random localized displacements, and (b) larger strains, ε_h = -0.05, exhibiting long-ranged displacements and structural inhomogeneities.

Lattice dynamics of MOF-5 at moderately large compressive strains

At ε_h = -0.015, the coupling of unstable optical modes with hydrostatic strain result in loss of elastic rigidity of MOF-5, as characterized by unstable transverse acoustic (TA) branches along various crystallographic directions (see Figure S6).

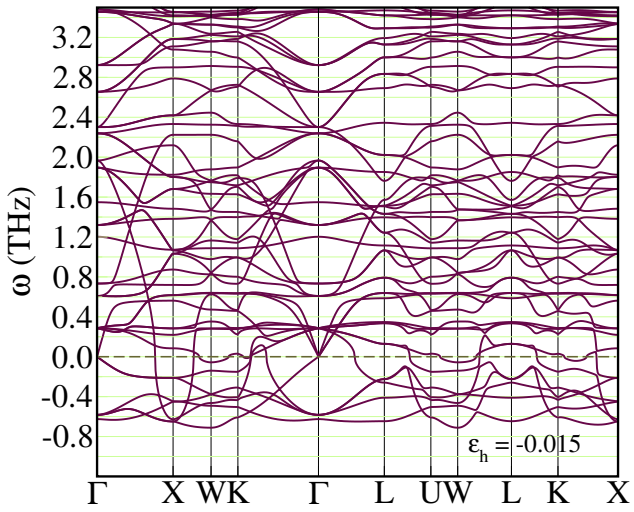

Figure S6: Low-frequency vibrational spectrum of compressed MOF-5 crystal, ε_h = -0.015, exhibiting instability of softest transverse acoustic (TA) branches and unstable optical modes.

MOF-5 structure

```
_audit_creation_method   'Generated by vasp2cif'
_space_group_IT_number           225
_symmetry_cell_setting           cubic
_symmetry_Int_Tables_number      225
_symmetry_space_group_name_Hall  '-F 4 2 3'
_symmetry_space_group_name_H-M   'F m -3 m'
_cell_length_a    18.4214482921
_cell_length_b    18.4214482921
_cell_length_c    18.4214482921
_cell_angle_alpha    60.0
_cell_angle_beta    60.0
_cell_angle_gamma    60.0
_atom_site_occupancy
Zn1   Zn   0.29359425   0.29359425   0.29359425   8.0
O9    O    0.25000000   0.25000000   0.25000000   1.0
O11   O    0.36680875   0.36680875   0.19492224   24.0
C35   C    0.38912961   0.38912961   0.11087038   12.0
C47   C    0.44640641   0.44640641   0.05359358   12.0
C59   C    0.47337519   0.47337519   0.09235429   24.0
H83   H    0.45194996   0.45194996   0.16437598   24.0
_symmetry_equiv_pos_as_xyz
'x, y, z'
'-x, -y, z'
'-x, y, -z'
'x, -y, -z'
'z, x, y'
'z, -x, -y'
'-z, -x, y'
'-z, x, -y'
'y, z, x'
'-y, z, -x'
```

'y, -z, -x'

'-y, -z, x'

'y, x, -z'

'-y, -x, -z'

'y, -x, z'

'-y, x, z'

'x, z, -y'

'-x, z, y'

'-x, -z, -y'

'x, -z, y'

'z, y, -x'

'z, -y, x'

'-z, y, x'

'-z, -y, -x'

'x, y+1/2, z+1/2'

'-x, -y+1/2, z+1/2'

'-x, y+1/2, -z+1/2'

'x, -y+1/2, -z+1/2'

'z, x+1/2, y+1/2'

'z, -x+1/2, -y+1/2'

'-z, -x+1/2, y+1/2'

'-z, x+1/2, -y+1/2'

'y, z+1/2, x+1/2'

'-y, z+1/2, -x+1/2'

'y, -z+1/2, -x+1/2'

'-y, -z+1/2, x+1/2'

'y, x+1/2, -z+1/2'

'-y, -x+1/2, -z+1/2'

'y, -x+1/2, z+1/2'

'-y, x+1/2, z+1/2'

'x, z+1/2, -y+1/2'

'-x, z+1/2, y+1/2'

'-x, -z+1/2, -y+1/2'

'x, -z+1/2, y+1/2'

'z, y+1/2, -x+1/2'

'z, -y+1/2, x+1/2'

'-z, y+1/2, x+1/2'

'-z, -y+1/2, -x+1/2'

'x+1/2, y, z+1/2'

'-x+1/2, -y, z+1/2'

'-x+1/2, y, -z+1/2'

'x+1/2, -y, -z+1/2'

'z+1/2, x, y+1/2'

'z+1/2, -x, -y+1/2'

'-z+1/2, -x, y+1/2'

'-z+1/2, x, -y+1/2'

'y+1/2, z, x+1/2'

'-y+1/2, z, -x+1/2'

'y+1/2, -z, -x+1/2'

'-y+1/2, -z, x+1/2'

'y+1/2, x, -z+1/2'

'-y+1/2, -x, -z+1/2'

'y+1/2, -x, z+1/2'

'-y+1/2, x, z+1/2'

'x+1/2, z, -y+1/2'

'-x+1/2, z, y+1/2'

'-x+1/2, -z, -y+1/2'

'x+1/2, -z, y+1/2'

'z+1/2, y, -x+1/2'

'z+1/2, -y, x+1/2'

'-z+1/2, y, x+1/2'

'-z+1/2, -y, -x+1/2'

'x+1/2, y+1/2, z'

'-x+1/2, -y+1/2, z'

'-x+1/2, y+1/2, -z'

'x+1/2, -y+1/2, -z'

'z+1/2, x+1/2, y'

'z+1/2, -x+1/2, -y'

'-z+1/2, -x+1/2, y'

'-z+1/2, x+1/2, -y'

'y+1/2, z+1/2, x'

'-y+1/2, z+1/2, -x'

'y+1/2, -z+1/2, -x'

'-y+1/2, -z+1/2, x'

'y+1/2, x+1/2, -z'

'-y+1/2, -x+1/2, -z'

'y+1/2, -x+1/2, z'

'-y+1/2, x+1/2, z'

'x+1/2, z+1/2, -y'

'-x+1/2, z+1/2, y'

'-x+1/2, -z+1/2, -y'

'x+1/2, -z+1/2, y'

'z+1/2, y+1/2, -x'

'z+1/2, -y+1/2, x'

'-z+1/2, y+1/2, x'

'-z+1/2, -y+1/2, -x'

'-x, -y, -z'

'x, y, -z'

'x, -y, z'

'-x, y, z'

'-z, -x, -y'

'-z, x, y'

'z, x, -y'

'z, -x, y'

'-y, -z, -x'

'y, -z, x'

'-y, z, x'

'y, z, -x'

'-y, -x, z'

'y, x, z'

'-y, x, -z'

'y, -x, -z'

'-x, -z, y'

'x, -z, -y'

'x, z, y'

'-x, z, -y'

'-z, -y, x'

'-z, y, -x'

'z, -y, -x'

'z, y, x'

'-x, -y+1/2, -z+1/2'

'x, y+1/2, -z+1/2'

'x, -y+1/2, z+1/2'

'-x, y+1/2, z+1/2'

'-z, -x+1/2, -y+1/2'

'-z, x+1/2, y+1/2'

'z, x+1/2, -y+1/2'

'z, -x+1/2, y+1/2'

'-y, -z+1/2, -x+1/2'

'y, -z+1/2, x+1/2'

'-y, z+1/2, x+1/2'

'y, z+1/2, -x+1/2'

'-y, -x+1/2, z+1/2'

'y, x+1/2, z+1/2'

'-y, x+1/2, -z+1/2'

'y, -x+1/2, -z+1/2'

'-x, -z+1/2, y+1/2'

'x, -z+1/2, -y+1/2'

'x, z+1/2, y+1/2'

'-x, z+1/2, -y+1/2'

'-z, -y+1/2, x+1/2'

'-z, y+1/2, -x+1/2'

'z, -y+1/2, -x+1/2'

'z, y+1/2, x+1/2'

'-x+1/2, -y, -z+1/2'

'x+1/2, y, -z+1/2'

'x+1/2, -y, z+1/2'

'-x+1/2, y, z+1/2'

'-z+1/2, -x, -y+1/2'

'-z+1/2, x, y+1/2'

'z+1/2, x, -y+1/2'

'z+1/2, -x, y+1/2'

'-y+1/2, -z, -x+1/2'

'y+1/2, -z, x+1/2'

'-y+1/2, z, x+1/2'

'y+1/2, z, -x+1/2'

'-y+1/2, -x, z+1/2'

'y+1/2, x, z+1/2'

'-y+1/2, x, -z+1/2'

'y+1/2, -x, -z+1/2'

'-x+1/2, -z, y+1/2'

'x+1/2, -z, -y+1/2'

'x+1/2, z, y+1/2'

'-x+1/2, z, -y+1/2'

'-z+1/2, -y, x+1/2'

'-z+1/2, y, -x+1/2'

'z+1/2, -y, -x+1/2'

'z+1/2, y, x+1/2'

'-x+1/2, -y+1/2, -z'

'x+1/2, y+1/2, -z'

'x+1/2, -y+1/2, z'

'-x+1/2, y+1/2, z'

'-z+1/2, -x+1/2, -y'

'-z+1/2, x+1/2, y'

'z+1/2, x+1/2, -y'

```
'z+1/2, -x+1/2, y'
'-y+1/2, -z+1/2, -x'
'y+1/2, -z+1/2, x'
'-y+1/2, z+1/2, x'
'y+1/2, z+1/2, -x'
'-y+1/2, -x+1/2, z'
'y+1/2, x+1/2, z'
'-y+1/2, x+1/2, -z'
'y+1/2, -x+1/2, -z'
'-x+1/2, -z+1/2, y'
'x+1/2, -z+1/2, -y'
'x+1/2, z+1/2, y'
'-x+1/2, z+1/2, -y'
'-z+1/2, -y+1/2, x'
'-z+1/2, y+1/2, -x'
'z+1/2, -y+1/2, -x'
'z+1/2, y+1/2, x'
```

References

(S1) Lock, N.; Wu, Y.; Christensen, M.; Cameron, L. J.; Peterson, V. K.; Bridgeman, A. J.; Kepert, C. J.; Iversen, B. B. Elucidating negative thermal expansion in MOF-5. *The Journal of Physical Chemistry C* **2010**, *114*, 16181–16186.

(S2) Li, H.; Eddaoudi, M.; O'Keeffe, M.; Yaghi, O. M. Design and synthesis of an exceptionally stable and highly porous metal-organic framework. *Nature* **1999**, *402*, 276–279.

(S3) Tranchemontagne, D. J.; Hunt, J. R.; Yaghi, O. M. Room temperature synthesis of metal-organic frameworks: MOF-5, MOF-74, MOF-177, MOF-199, and IRMOF-0. *Tetrahedron* **2008**, *64*, 8553 – 8557.